

Cite this: *Chem. Commun.*, 2017, 53, 4605Received 14th March 2017,  
Accepted 31st March 2017

DOI: 10.1039/c7cc01944k

rsc.li/chemcomm

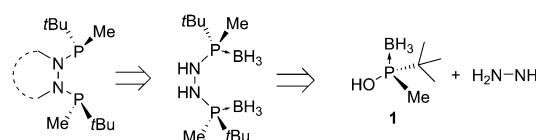
# P-Stereogenic bisphosphines with a hydrazine backbone: from N–N atropoisomerism to double nitrogen inversion†

Amparo Prades,<sup>ib</sup><sup>a</sup> Samuel Núñez-Pertíñez,<sup>ib</sup><sup>a</sup> Antoni Riera<sup>ib</sup><sup>\*ab</sup> and Xavier Verdager<sup>ib</sup><sup>\*ab</sup>

The synthesis of P-stereogenic bisphosphine ligands starting from a phosphinous acid chiral synthon and hydrazine is reported. The dialkylation of the hydrazine backbone yielded atropo- and nitrogen inversion isomers which are in slow exchange. The crystallization of one of the isomers allowed us to study the reaction kinetics of the equilibria. The new ligands were tested in the Rh catalysed asymmetric hydrogenation of various benchmark substrates attaining up to 99% ee.

Developing active and selective chiral catalysts is highly relevant for the chemical and pharmaceutical industries.<sup>1</sup> “Ligand engineering” is a key approach to generate new and more efficient catalytic systems. Among the different types of ligand, chiral phosphines have made a key contribution to asymmetric catalysis, which is one of the most effective synthetic methodologies by which to obtain optically pure compounds.<sup>2</sup> Since the pioneering work of Kagan with DIOP<sup>3</sup> and Knowles with DIPAMP,<sup>4</sup> a large number of chiral bisphosphine ligands have been reported. Among these, P-stereogenic phosphines have proved to be a privileged class of ligands.<sup>5,6</sup> Despite enormous advances in this field, P-stereogenic ligands are usually made through a lengthy multistep synthesis. Thus, the search for cost efficient synthesis of optically pure P-stereogenic ligands is of key importance.

Our group has recently reported procedures for the synthesis of optically pure P-stereogenic *tert*-butylmethylphosphinous acid borane **1**.<sup>7</sup> This fragment is highly versatile and has allowed access to *C*<sub>1</sub> symmetric MaxPHOS<sup>8</sup> and MaxPHOX<sup>9</sup> ligands. In this



Scheme 1 Strategy developed for the synthesis of P-stereogenic *C*<sub>2</sub> bisphosphines with a hydrazine backbone.

context, we addressed whether our methodology could also be amenable for the rapid and efficient synthesis of ligands with *C*<sub>2</sub> symmetry. We hypothesized that the coupling of hydrazine to the activated phosphinous acid **1** could provide nitrogen analogs of bis-P\* type ligands (Scheme 1).<sup>10</sup> Here we report the synthesis of two borane-protected P-stereogenic hydrazine bisphosphine ligands derived from hydrazine and **1**. In solution, these ligands are present as a mixture of atropo- and nitrogen inversion isomers in slow exchange. These ligands were also tested in the Rh catalyzed asymmetric hydrogenation, attaining selectivities up to 99% ee.

Initially, in order to identify all possible intermediates, a sequential synthesis was performed, starting from **1** and Boc-hydrazine (Scheme 2). Phosphinous acid **1** was activated with Ms<sub>2</sub>O following our procedure.<sup>7c</sup> The reaction with *tert*-butyl carbazate at –20 °C provided hydrazine **2** (58%) in an S<sub>N</sub>2@P-type process. The reaction was stereospecific and occurred with inversion of configuration at the phosphorus center. The Boc protecting group was removed using anhydrous HCl in MeOH to yield phosphino hydrazine **3** in 72% yield. From **3**, a second phosphinous acid coupling provided bisphosphine **4** in 56% yield. Satisfactory stereocontrol was observed throughout the syntheses, and *meso*-**4** was not detected. We next attempted the one-pot preparation of **4** starting from hydrazine and 2 equivalents of phosphinous acid **1**. We observed that **4** was assembled efficiently in one step with 82% yield.

To improve the stability of the resulting ligands, we derivatized **4** by alkylation on both nitrogen atoms.<sup>11</sup> The methylation of **4** was achieved by deprotonating hydrazine nitrogen atoms with sodium hydride and adding an excess of methyl iodide

<sup>a</sup> Institute for Research in Biomedicine (IRB Barcelona), The Barcelona Institute of Science and Technology, Baldri Reixac 10, E-08028, Spain.

E-mail: antoni.riera@irbbarcelona.org, xavier.verdager@irbbarcelona.org;

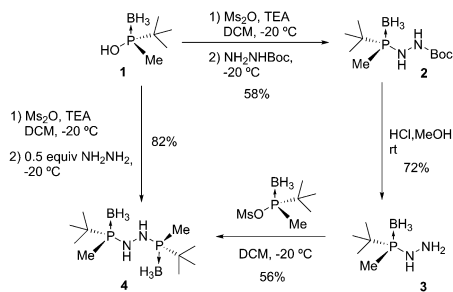
Tel: +34 934034813

<sup>b</sup> Dept. Química Inorgànica i Orgànica, Secció de Química Orgànica,

Universitat de Barcelona, Martí i Franquès 1, E-08028 Barcelona, Spain

† Electronic supplementary information (ESI) available: Experimental procedures, characterization data and NMR spectra for new compounds; crystallographic data file in CIF format. CCDC 1533430–1533432. For ESI and crystallographic data in CIF or other electronic format see DOI: 10.1039/c7cc01944k

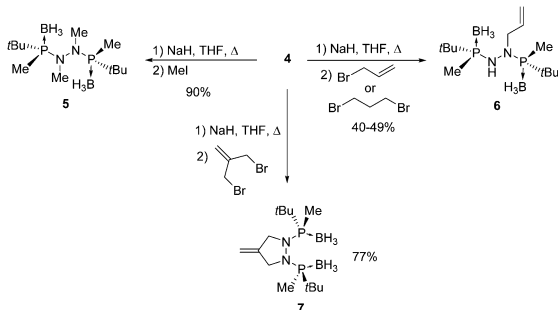




Scheme 2 Sequential and direct synthesis of the  $C_2$  bisphosphine hydrazine **4**.

at 55 °C (Scheme 3). The dimethyl derivative **5** was isolated in 90% yield. When allyl bromide was used as the alkylating agent, only monoalkylated product **6** was obtained in moderate yield (49%). The dialkylated product was not observed, even when the reaction temperature was increased and the solvent changed. At this stage, a large number of electrophiles were also tested; however, dialkylation products were not detected. A cyclization reaction was attempted with 1,3-dibromopropane as the alkylating agent. However, the reaction did not afford the expected pyrazolidine ring. The NMR spectra were in concordance with the formation of **6**, which results from the monoalkylation of **4** followed by base-promoted elimination of HBr. Finally, we deduced that, by using 3-bromo-2-bromomethyl-1-propene, we could avoid the undesired E2 type reaction. Indeed, using this electrophile, the cyclization occurred swiftly, providing the corresponding pyrazolidine **7** in 77% yield.

$^1\text{H}$  NMR showed that crystalline **5** was present as a single compound; however, upon dissolution, it rapidly equilibrated to a 1:1 mixture of isomers. Analysis of **5** by thin-layer chromatography (TLC) on silica provided two spots with retention factors of 0.3 and 0.5 (hexane:AcOEt 8:2). However, when the reaction crude product was eluted through a  $\text{SiO}_2$  flash column, the two substances were equally present in all the fractions. 2D-TLC analysis showed that, even in a quick elution, the two products could not be isolated. The system re-equilibrated a second time, with a new set of spots on the TLC appearing for every single spot in the first elution. This observation suggested that **5** was present as a mixture of two isomers in slow exchange. A variable temperature  $^1\text{H}$ -NMR experiment of a solution of **5** in  $\text{DMSO-d}_6$  was performed at 25, 40 and 70 °C. During the experiment, the signals



Scheme 3 N-Alkylation of the hydrazine backbone.

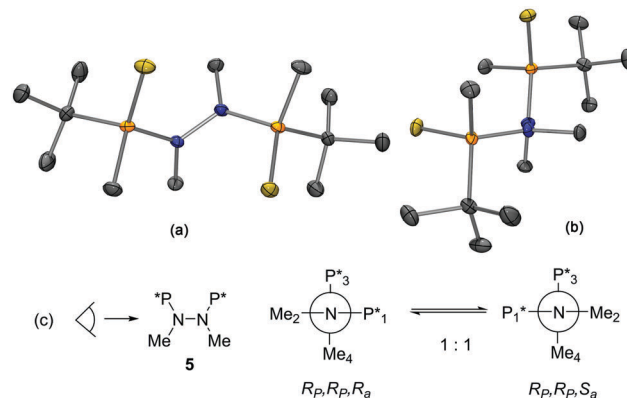


Fig. 1 X-Ray structure of  $(R_p,R_p,S_a)$ -**5**. (a) Perspective and (b) Newman projection through the N–N axis. ORTEP drawing showing thermal ellipsoids at 50% probability. (c) Newman projections for the equilibrium of compound **5**. In solution, **5** is present as a mixture of diastereomeric N–N atropoisomers. In the solid state, only the  $(R_p,R_p,S_a)$  atropoisomer is observed.

corresponding to the protons of the  $\text{NCH}_3$  groups of the two species got closer, but total coalescence was not observed, and at 100 °C the sample decomposed.

The X-ray structure of **5** is depicted in Fig. 1.<sup>12</sup> The sum of the angles around the trisubstituted nitrogen atoms added up to 360.0 and 359.9°, which indicates that the N atoms were completely planar. The view through the N–N axis shows how the two N planes are almost perpendicular, the P–N–N–P torsion angle being 98.0°. All these findings sustain that the two species observed in solution are atropoisomers that arise from the hampered rotation around the N–N bond caused by the increased steric hindrance of the phosphorus groups (Fig. 1c).<sup>13</sup> Because of the presence of P-stereogenic centers, the new axial chirality leads to two distinct diastereoisomers  $(R_p,R_p,R_a)$ -**5** and  $(R_p,R_p,S_a)$ -**5**, which can be observed as two sets of signals in the  $^1\text{H}$  NMR spectrum. As  $(R_p,R_p,S_a)$ -**5** was the only atropoisomer present in the solid state, a kinetics study was performed to determine the activation energy of the equilibrium between the two atropoisomers.<sup>14</sup> Crystals of  $(R_p,R_p,S_a)$ -**5** were dissolved in deuterated chloroform in a NMR tube, and successive  $^1\text{H}$ -NMR spectra were collected at specific times.<sup>15</sup> After approximately 30 min, the concentrations of the two atropoisomers were the same. The kinetic data followed a first order profile for the  $S_a/R_a$  equilibrium with kinetic constant  $k_1 = k_{-1} = 1.47 \times 10^{-3} \text{ s}^{-1}$ , and a  $\Delta G^\ddagger$  of  $21 \text{ kcal mol}^{-1} = 88 \text{ kJ mol}^{-1}$ . It is commonly assumed that the free energy barrier between conformational and configurational isomers is  $100 \text{ kJ mol}^{-1}$ , which means that if the interconversion barrier is higher than  $100 \text{ kJ mol}^{-1}$ , isomers can be isolated. This finding is in agreement with the observation that atropoisomers  $(R_p,R_p,S_a)$ -**5** and  $(R_p,R_p,R_a)$ -**5** can be detected by TLC and NMR but cannot be isolated using chromatographic techniques at room temperature.

Similar behavior was observed for pyrazolidine **7**. When the crude product was eluted through a  $\text{SiO}_2$  flash column, two isomers in a 1:1 ratio could be clearly separated and isolated,



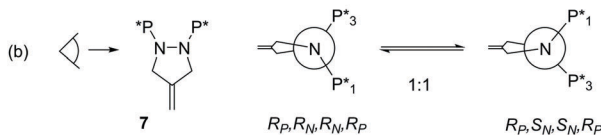
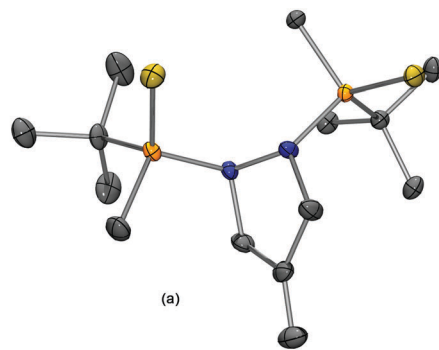
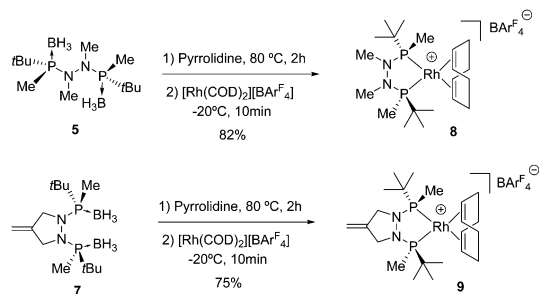


Fig. 2 (a) X-Ray structure of  $(R_P,R_N,R_N,R_P)$ -**7**. ORTEP drawing showing one of the two independent molecules in the unit cell (thermal ellipsoids at 50% probability). (b) Newman projections of the equilibrium for compound **7**. In solution, compound **7** is present as a mixture of diastereomers resulting from a double nitrogen inversion.

as confirmed by  $^1\text{H}$  NMR. However, the samples underwent equilibration within 24 h to the initial 1:1 mixture.  $^1\text{H}$  NMR analysis showed that, upon crystallization, the crystals contained a single isomer of **7**. X-ray diffraction analysis revealed that the unit cell contained two independent molecules of  $(R_P,R_N,R_N,R_P)$ -**7**, both bearing the phosphorus atoms with the *R* configuration (Fig. 2).<sup>12</sup> The sum of the angles around the nitrogen centers added up to  $348.6/351.8^\circ$  and  $336.0/334.7^\circ$ . The geometrical constraints imposed by the five-membered ring force the nitrogen atoms to adopt a trigonal pyramidal geometry, with the bulky phosphorus groups lying at opposite sides of the pyrazolidine ring, with a P–N–N–P torsion angle of  $122.8/118.6^\circ$ . In this circumstance, the isomerization equilibrium can more accurately be described as a double nitrogen inversion rather than atropisomerism (Fig. 2b). The kinetics of the isomerization of **7** were also studied by  $^1\text{H}$  NMR. Upon dissolution of the pure isomers in  $\text{CDCl}_3$ , almost complete isomerization was observed after 24 h.<sup>15</sup> The kinetic constants were calculated to be  $k_1 = k_{-1} = 1.04 \times 10^{-5} \text{ s}^{-1}$ , with a  $\Delta G^\ddagger$  of  $24 \text{ kcal mol}^{-1}$  ( $100.4 \text{ kJ mol}^{-1}$ ). These findings indicate that the energy barrier between  $(R_P,R_N,R_N,R_P)$ -**7** and  $(R_P,S_N,S_N,R_P)$ -**7** was at the border between configurational and conformational isomers, in agreement with the experimental observations.

To date, the use of hydrazine as a backbone for non-chiral and chiral diphosphines and in catalysis has met limited success.<sup>16</sup> For instance, chiral hydrazine diphosphoramidites have been described, and their use in the rhodium-catalyzed hydrogenation of *Z*-MAC afforded up to 93% enantiomeric excess.<sup>17</sup> With the aim to study the ability of ligands **5** and **7** in catalysis, we proceeded to test them in the Rh catalyzed asymmetric hydrogenation of standard test substrates.

Heating **5** and **7** with neat pyrrolidine at  $80^\circ\text{C}$  for 2 h resulted in complete borane deprotection.<sup>18</sup> After pyrrolidine removal, the crude ligand was reacted with  $[\text{Rh}(\text{COD})_2][\text{BARF}_4]$  to



Scheme 4 Borane removal and complexation to Rh(I).

furnish the desired cationic complexes **8** and **9** (Scheme 4).<sup>12,19,20</sup> Asymmetric hydrogenation with catalysts **8** and **9** at 3 bar of  $\text{H}_2$  and 1 mol% of catalyst loading took place with complete conversions (Table 1). In the reduction of methyl  $\alpha$ -acetamidoacrylate (MAA) catalyst **9**, with a pyrazolidine backbone, provided better enantioselectivity (98% vs. 95% ee, Table 1, entries 1 and 2). (*Z*)-Methyl  $\alpha$ -acetamido-3-phenylacrylate (*Z*-MAC) was hydrogenated to full conversion and almost complete selectivity (99% ee) with both catalysts (Table 1, entries 3 and 4). The novel complexes were also active in the hydrogenation of *N*-(1-phenylvinyl)acetamide (PVA) yielding full conversion and enantiomeric excess up to 97% (Table 1, entries 6 and 7). Reducing the amount of the catalyst to 0.1 mol% of **9** did not have an adverse effect on the selectivity of the reaction (Table 1, entry 8). Finally, catalyst **9** proved to be highly active and selective in the hydrogenation of dimethyl itaconate (DMI), affording the product with full stereocontrol (99% ee, Table 1, entry 9). When the catalyst loading was reduced to 0.02 mol%, a slight decrease in selectivity was observed, and dimethyl itaconate was isolated in 97% enantiomeric excess (Table 1, entry 10).

In summary, we report a new class of P-stereogenic  $C_2$ -symmetric ligands with a hydrazine backbone. The ligands were assembled from hydrazine and optically pure *tert*-butylmethylphosphinous acid in a rapid and efficient synthesis.

Table 1 Asymmetric hydrogenation using catalysts **8** and **9**<sup>a</sup>

Entry	Catalyst (S/C)	Substrate <sup>b</sup>	Conv. <sup>c</sup> (%)	ee <sup>d</sup> (%)
1	<b>8</b> (100)	MAA	99	95
2	<b>9</b> (100)	MAA	99	98
3	<b>8</b> (100)	<i>Z</i> -MAC	99	99
4	<b>9</b> (100)	<i>Z</i> -MAC	99	99
5	<b>9</b> (100)	<i>Z</i> -MATC	99	99
6	<b>8</b> (100)	PVA	99	95
7	<b>9</b> (100)	PVA	99	97
8	<b>9</b> (1000)	PVA	99	97
9	<b>9</b> (100)	DMI	99	99
10	<b>9</b> (5000)	DMI	99	97

<sup>a</sup> Reaction conditions: 0.7 mmol of substrate and 1 mol% of catalyst in dry MeOH were placed in a Büchi 250 Miniclave. The system was charged with 3.0 bar of hydrogen gas and the mixture was stirred for 12 h at r.t. <sup>b</sup> Methyl  $\alpha$ -acetamidoacrylate (MAA), (*Z*)-methyl  $\alpha$ -acetamido-3-phenylacrylate (*Z*-MAC), (*Z*)-methyl  $\alpha$ -acetamido-3-(3,4,5-trimethylphenyl)acrylate (*Z*-MATC), *N*-(1-phenylvinyl)acetamide (PVA), dimethyl itaconate (DMI). <sup>c</sup> Conversion was determined by  $^1\text{H}$  NMR of the crude reaction mixture. <sup>d</sup> Enantiomeric excess determined by chiral GC or HPLC.



The borane-protected ligands **5** and **7** were present as a mixture of atropo- and nitrogen-inversion isomers which are in slow exchange in solution. The nature of such an equilibrium was studied through a combination X-ray crystallography and reaction kinetics. The new ligands were tested in the Rh-catalyzed asymmetric hydrogenation of benchmark substrates demonstrating that ligands with a hydrazine backbone can show excellent catalytic performance.

We thank the MINECO (CTQ2014-56361-P) and IRB Barcelona for financial support. A. P. thanks AGAUR for a Beatriu de Pinós fellowship. IRB Barcelona is the recipient of a Severo Ochoa Award of Excellence from MINECO (Government of Spain).

## Notes and references

- (a) *Asymmetric Catalysis On Industrial Scale: Challenges, Approaches and Solutions*, ed. H. A. Blaser and H. J. Federsel, Wiley-VCH, Weinheim, Germany, 2010; (b) N. B. Johnson, I. C. Lennon, P. H. Moran and J. A. Ramsden, *Acc. Chem. Res.*, 2007, **40**, 1291; (c) L. A. Saudan, *Acc. Chem. Res.*, 2007, **40**, 1309; (d) H. Shimizu, I. Nagasaki, K. Matsumura, N. Sayo and T. Saito, *Acc. Chem. Res.*, 2007, **40**, 1385; (e) A. M. Palmer and A. Zanotti-Gerosa, *Curr. Opin. Drug Discovery Dev.*, 2010, **13**, 698; (f) P. Etayo and A. Vidal-Ferran, *Chem. Soc. Rev.*, 2013, **42**, 728.
- (a) *Phosphorus Ligands in Asymmetric Catalysis*, ed. A. Börner, Wiley-VCH, Weinheim, Germany, 2008; (b) W. J. Tang and X. M. Zhang, *Chem. Rev.*, 2003, **103**, 3029; (c) W. Zhang, Y. Chi and X. Zhang, *Acc. Chem. Res.*, 2007, **40**, 1278; (d) G. Erre, S. Enthaler, K. Junge, S. Gladiali and M. Beller, *Coord. Chem. Rev.*, 2008, **252**, 471; (e) H.-U. Blaser, B. Pugin, F. Spindler and M. Thommen, *Acc. Chem. Res.*, 2007, **40**, 1240; (f) H. Fernández-Pérez, P. Etayo, A. Panossian and A. Vidal-Ferran, *Chem. Rev.*, 2011, **111**, 2119; (g) O. I. Kolodiazny, *Phosphorus Chemistry I: Asymmetric Synthesis and Bioactive Compounds*, in *Topics in Current Chemistry*, ed. J. Montchamp, 2015, vol. 360, p. 161.
- H. B. Kagan and T. P. Dang, *J. Am. Chem. Soc.*, 1972, **94**, 6429.
- W. S. Knowles, M. J. Sabacky, B. D. Vineyard and D. J. Weinkauff, *J. Am. Chem. Soc.*, 1975, **97**, 2567.
- For reviews on P-stereogenic phosphorus compounds, see: (a) A. Grabulosa, J. Granell and G. Muller, *Coord. Chem. Rev.*, 2007, **251**, 25; (b) O. I. Kolodiazny, *Top. Curr. Chem.*, 2015, **360**, 1616; (c) M. Dutartre, J. Bayardon and S. Jugé, *Chem. Soc. Rev.*, 2016, **45**, 5771.
- For selected applications of this family of phosphines and other P-stereogenic phosphines, see: (a) G. Xu, W. Fu, G. Liu, C. H. Senanayake and W. Tang, *J. Am. Chem. Soc.*, 2014, **136**, 570; (b) I.-H. Chen, L. Yin, W. Itano, M. Kanai and M. Shibasaki, *J. Am. Chem. Soc.*, 2009, **131**, 11664; (c) H. Ito, T. Okura, K. Matsuura and M. Sawamura, *Angew. Chem., Int. Ed.*, 2010, **49**, 560; (d) X. Wang and S. L. Buchwald, *J. Am. Chem. Soc.*, 2011, **133**, 19080; (e) Q. Hu, Z. Zhang, Y. Liu, T. Imamoto and W. Zhang, *Angew. Chem., Int. Ed.*, 2015, **54**, 2260; (f) Y. Shibata and K. Tanaka, *J. Am. Chem. Soc.*, 2009, **131**, 12552; (g) A. Yanagisawa, S. Takeshita, Y. Izumi and K. Yoshida, *J. Am. Chem. Soc.*, 2010, **132**, 5328; (h) H. Li, K. M. Belyk, J. Yin, Q. Chen, A. Hyde, Y. Ji, S. Oliver, M. T. Tudge, L.-C. Campeau and K. R. Campos, *J. Am. Chem. Soc.*, 2015, **137**, 13728; (i) R. Tan, X. Zheng, B. Qu, C. A. Sader, K. R. Fandrick, C. H. Senanayake and X. Zhang, *Org. Lett.*, 2016, **18**, 3346.
- (a) M. Revés, C. Ferrer, T. León, S. Doran, P. Etayo, A. Vidal-Ferran, A. Riera and X. Verdaguer, *Angew. Chem., Int. Ed.*, 2010, **49**, 9452; (b) T. León, A. Riera and X. Verdaguer, *J. Am. Chem. Soc.*, 2011, **133**, 5740; (c) S. Orgué, A. Flores, M. Biosca, O. Pàmies, M. Diéguez, A. Riera and X. Verdaguer, *Chem. Commun.*, 2015, **51**, 17548.
- E. Cristóbal-Lecina, P. Etayo, S. Doran, M. Revés, P. Martín-Gago, A. Grabulosa, A. R. Costantino, A. Vidal-Ferran, A. Riera and X. Verdaguer, *Adv. Synth. Catal.*, 2014, **356**, 795.
- E. Salomó, S. Orgué, A. Riera and X. Verdaguer, *Angew. Chem., Int. Ed.*, 2016, **55**, 7988.
- (a) T. Imamoto, J. Watanabe, Y. Wada, H. Masuda, H. Yamada, H. Tsuruta, S. Matsukawa and K. Yamaguchi, *J. Am. Chem. Soc.*, 1998, **120**, 1635; (b) I. D. Gridnev, M. Yasutake, N. Higashi and T. Imamoto, *J. Am. Chem. Soc.*, 2001, **123**, 5268; (c) I. D. Gridnev, Y. Yamanoi, N. Higashi, H. Tsuruta, M. Yasutake and T. Imamoto, *Adv. Synth. Catal.*, 2001, **343**, 118.
- A. N. Kornev, N. V. Belina, V. V. Sushev, G. K. Fukin, E. V. Baranov, Y. A. Kurskiy, A. I. Poddelskii, G. A. Abakumov, P. Loennecke and E. Hey-Hawkins, *Inorg. Chem.*, 2009, **48**, 5574.
- CCDC 1533430 (5), 1533431 (7) and 1533432 (9).
- To our knowledge there are almost no examples of N–N atropo-isomerism equilibria. For examples of non-biaryl atropoisomers, see: E. Kumarasamy, R. Raghunathan, M. P. Sibi and J. Sivaguru, *Chem. Rev.*, 2015, **115**, 11239.
- Since both nitrogen atoms are completely planar, the new source of chirality in **5** is an N–N chiral axis. However, it is possible that in the process of isomerization either one or the two nitrogen atoms adopt a pyramidal structure.
- See the ESI† for full details.
- (a) B. R. Aluri, N. Peulecke, B. H. Müller, S. Peitz, A. Spannenberg, M. Hapke and U. Rosenthal, *Organometallics*, 2010, **29**, 226; (b) A. Bollmann, K. Blann, J. T. Dixon, F. M. Hess, E. Killian, H. Maumela, D. S. McGuinness, D. H. Morgan, A. Neveling, S. Otto, M. Overett, A. M. Z. Slawin, P. Wasserscheid and S. Kuhlmann, *J. Am. Chem. Soc.*, 2004, **126**, 14712; (c) A. M. Z. Slawin, M. Wainwright and J. D. Woollins, *J. Chem. Soc., Dalton Trans.*, 2002, 513.
- L. Eberhardt, D. Armspach, D. Matt, B. Oswald and L. Toupet, *Org. Biomol. Chem.*, 2007, **5**, 3340.
- Compound **4** was deboronated in the same conditions. See the ESI† for experimental details and NMR data on the resulting secondary diphosphazene.
- Initial coordination studies were performed using  $[\text{Rh}(\text{COD})_2][\text{BF}_4]$  as metal precursor but a mixture of the desired product and a cationic rhodium complex bearing two bisphosphine ligands was obtained without possibility to separate them.
- Complex **9** does not show any dynamic behavior and in solution behaves as single  $C_2$ -symmetric compound. X-ray analysis (ESI†) shows a bite-angle of  $82.2^\circ$  which is slightly smaller than the corresponding carbon analog bisP\*-Rh ( $83.3^\circ$ ), see ref. 10.

